

Paterno–Büchi Coupling of (Diaryl)acetylenes and Quinone via Photoinduced Electron Transfer

E. Bosch, S. M. Hubig, and J. K. Kochi*

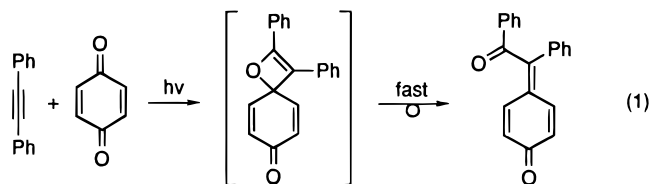
Contribution from the Chemistry Department, University of Houston, Houston, Texas 77204-5641

Received August 7, 1997

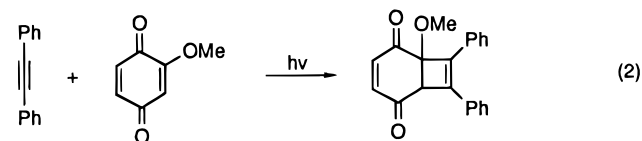
Abstract: Photoinduced coupling of an acetylene with a quinone in two wavelength regions (λ_{DB} and λ_{CT}) can be regioselective to yield a single quinone methide adduct when various diarylacetylenes (**DA**) and 2,6-dichlorobenzoquinone (**DB**) are used. Thus, the direct photoexcitation of **DB** at $\lambda_{DB} = 355$ nm or the specific activation of the 1:1 electron donor–acceptor complex [**DA,DB**] at $\lambda_{CT} = 532$ nm both lead to the transient ion-radical pair [**DA**^{•+},**DB**^{•-}], which is established by time-resolved (ps,ns) spectroscopy. Competition between back electron transfer (k_{BET}) and ion-radical pair collapse (k_C) to the distonic adduct **DA-DB**, as described in Schemes 1 and 2, limits the quantum yields for both photochemical processes in Table 4. The biradical nature of the distonic adduct in Scheme 3 accommodates the various facets of acetylene reactivity and unique regioselectivity to yield the same quinone methide by both actinic processes. In a more general context, the electron-transfer mechanism established by the charge-transfer excitation of [**DA,DB**] provides compelling evidence that the Paterno–Büchi coupling (by direct excitation of **DB**) can proceed via the same sequence of reactive intermediates.

Introduction

The photoinduced [2+2] cycloaddition of an olefin to a carbonyl center has become a convenient methodology for oxetane preparation with high regio- and stereoselectivities.^{1,2} As a result, the various synthetic and mechanistic aspects of this transformation, also known as the Paterno–Büchi reaction,³ have been the subject of numerous reviews.^{1,2,4–6} Most importantly, the scope has been extended over the years to include enones^{4,7} and quinones^{4,8} as the carbonyl component and alkenes, dienes, and acetylenes as the olefinic counterpart.^{4,9,10} As an example of the latter, the photocoupling of diphenylacetylene with *p*-benzoquinone⁹ leads to the corresponding quinone methide in excellent yield via the labile oxetene formed by [2+2] cycloaddition:^{10,11}



Since such quinone methides are bright yellow, the more recent applications of this transformation have been directed to the preparation of highly colored extended conjugated systems for industrial applications.¹² Interestingly, the analogous combination with the simple presence of a methoxy group (as in methoxy-*p*-benzoquinone) under essentially the same conditions leads to [2+2] cycloaddition at the C=C center:¹³



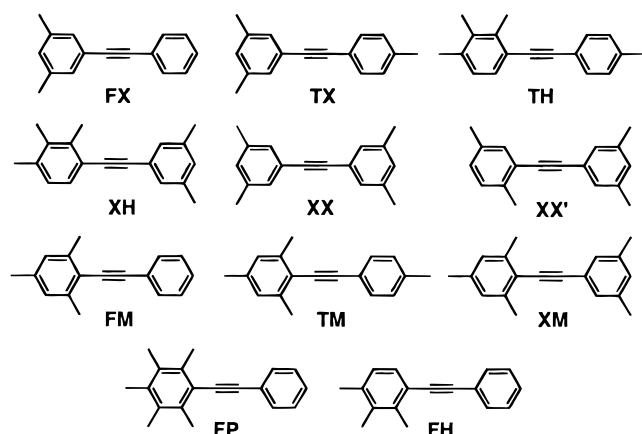
The divergent photochemical pathways in eqs 1 and 2 have been attributed to different excited states—benzoquinone proceeding via the oxygen-centered reactivity of the $n-\pi^*$ state^{9b} and methoxybenzoquinone proceeding via the carbon-centered reactivity of the $\pi-\pi^*$ state.¹³ However, the clear sequence of reaction steps for either pathway, i.e. oxetane or cyclobutane formation, has not been forthcoming. Whereas the formation of a 1,4-biradical as a crucial intermediate prior to cyclization is generally included in all postulated mechanisms,^{1,2,4–7} the role of other reactive intermediates such as exciplexes¹⁴ and

- (1) Demuth, M.; Mikhail, G. *Synthesis* **1989**, 145–162.
 (2) Porco, J. A.; Schreiber, S. L. In *Comprehensive Organic Synthesis*; Trost, B. M., Fleming, I., Paquette, L. A., Eds.; Pergamon: New York, 1991; Vol. 5, p 151.
 (3) (a) Paterno, E.; Chieffi, G. *Gazz. Chim. Ital.* **1909**, 39, 341. (b) Büchi, G.; Inman, C. G.; Lipinsky, E. S. *J. Am. Chem. Soc.* **1954**, 76, 4327.
 (4) Griesbeck, A. G. In *CRC Handbook of Organic Photochemistry and Photobiology*; Horspool, W. M., Song, P.-S., Eds.; CRC Press: Boca Raton, FL, 1995; p 522.
 (5) Arnold, D. R. *Adv. Photochem.* **1968**, 6, 301.
 (6) (a) Creed, D. in ref 4, p 737ff. (b) Jones, G., II In *Organic Photochemistry*; Padwa, A., Ed.; Dekker: New York, 1981; Vol. 5, p 1.
 (7) Schuster, D. I.; Lem, G.; Kaprinidis, N. A. *Chem. Rev. (Washington, D.C.)* **1993**, 93, 3.
 (8) (a) Bryce-Smith, D.; Gilbert, A. *Proc. Chem. Soc.* **1964**, 87. (b) Bryce-Smith, D.; Gilbert, A. *Tetrahedron Lett.* **1964**, 3471. (c) Xu, J.-H.; Song, Y.-L.; Zhang, Z.-G.; Wang, L.-C.; Xu, J.-W. *Tetrahedron* **1994**, 50, 1199.
 (9) (a) Zimmerman, H. E.; Craft, L. *Tetrahedron Lett.* **1964**, 2131. (b) Bryce-Smith, D.; Fray, G. I.; Gilbert, A. *Tetrahedron Lett.* **1964**, 2137.
 (10) (a) Bartrop, J. A.; Hesp, B. *J. Chem. Soc. (C)* **1967**, 1625. (b) Farid, S.; Kothe, W.; Pfundt, G. *Tetrahedron Lett.* **1968**, 4147. (c) Pappas, S. P.; Portnoy, N. A. *J. Org. Chem.* **1968**, 33, 2200.
 (11) Oxetenes are short-lived, but can exhibit lifetimes of up to several hours depending on the temperature. See: (a) Friedrich, L. E.; Bower, J. D. *J. Am. Chem. Soc.* **1973**, 95, 6869. (b) Friedrich, L. E.; Lam, P. Y.-S. *J. Org. Chem.* **1981**, 46, 306. (c) Friedrich, L. E.; Schuster, G. B. *J. Am. Chem. Soc.* **1971**, 93, 4602.

- (12) (a) Kim, S. S.; Kim, A. R.; Cho, I. H.; Shim, S. C. *Bull. Korean Chem. Soc.* **1989**, 10, 57. (b) Kim, S. S.; O, K. J.; Shim, S. C. *Bull. Korean Chem. Soc.* **1994**, 15, 270.

- (13) Pappas, S. P.; Pappas, B. C.; Portnoy, N. A. *J. Org. Chem.* **1969**, 34, 520.

Chart 1



ion-radical pairs^{15,16} is still controversial. In particular, the question remains open as to whether ion-radical pairs (i.e. carbonyl anion and olefin cation radicals which have been directly observed in the photocyclization of various carbonyl/olefin combinations^{15,16}) actually represent active precursors to the 1,4-biradical or are merely innocent bystanders. To address this question, we focused our studies on the efficient generation of the transient ion-radical pair for the photoinduced coupling in eq 1 by exploiting the unambiguous charge-transfer (CT) activation of the electron donor–acceptor complex.¹⁷ We chose a series of polymethylated tolane derivatives (with a range of dimethylphenyl to pentamethylphenyl moieties) in order to provide different reactivities and steric environments sufficient to delineate the regioselectivity of the Paterno–Büchi coupling. The diarylacetylenes shown in Chart 1 were prepared by the palladium-catalyzed coupling of arylacetylenes with iodoarenes¹⁸ (see the Experimental Section), and the acronyms reflect the pattern of methyl substitution on each of the phenyl groups, i.e. **F** = phenyl, **T** = tolyl, **X** = *m*-xylyl, **X'** = *p*-xylyl, **H** = hemimellityl, **M** = mesityl, and **P** = pentamethylphenyl with 0, 1, 2, 3, 4 or 5 methyl substituents. The 2,6-dichloro-substituted benzoquinone (**DB**) was chosen as the carbonyl component for the following reasons: (i) The well-defined absorption band of **DB** ($\lambda_{\max} = 340$ nm tailing to 500 nm) allows selective photoexcitation in the spectral region ($\lambda_{\text{exc}} > 410$ nm) where the tolanes do not absorb. The resulting long-lived triplet quinone¹⁹ (**DB*** with a microsecond lifetime²⁰ and a reduction potential of $E_{\text{red}} \sim 2$ V vs SCE²¹) presents the opportunity for an efficient (diffusional) electron transfer.²² (ii) Chloro-substituted benzoquinones as electron acceptors are capable of forming ground-state electron donor–acceptor (EDA) complexes, especially with various methylated benzenoid donors.²³

(14) (a) Caldwell, R. A.; Hrcir, D. C.; Muñoz, T., Jr.; Unett, D. J. *J. Am. Chem. Soc.* **1996**, *118*, 8741. (b) Caldwell, R. A.; Sovocool, G. W.; Gajewski, R. P. *J. Am. Chem. Soc.* **1973**, *95*, 2549. (c) Schore, N. E.; Turro, N. J. *J. Am. Chem. Soc.* **1975**, *97*, 2482.

(15) (a) Freilich, S. C.; Peters, K. S. *J. Am. Chem. Soc.* **1985**, *107*, 3819. (b) Freilich, S. C.; Peters, K. S. *J. Am. Chem. Soc.* **1981**, *103*, 6255. (c) Gersdorf, J.; Mattay, J.; Görner, H. *J. Am. Chem. Soc.* **1987**, *109*, 1203. (d) Griesbeck, A. G.; Mauder, H.; Stadtmüller, S. *Acc. Chem. Res.* **1994**, *27*, 70.

(16) Eckert, G.; Goez, M. *J. Am. Chem. Soc.* **1994**, *116*, 11999.

(17) Time-resolved spectroscopy has established charge-transfer excitation to effect the transfer of an electron from the donor to the acceptor within 500 fs. See: Wynne, K.; Galli, C.; Hochstrasser, R. M. *J. Chem. Phys.* **1994**, *100*, 4797.

(18) Takahashi, S.; Kuroyama, Y.; Sonogashira, K.; Hagihara, N. *Synthesis* **1980**, 627.

(19) Photoexcitation of quinones generates the triplet excited state within 10 ps. See: Hubig, S. M.; Bockman, T. M.; Kochi, J. K. *J. Am. Chem. Soc.* **1997**, *119*, 2926.

(20) Gschwind, R.; Haselbach, E. *Helv. Chim. Acta* **1979**, *62*, 941.

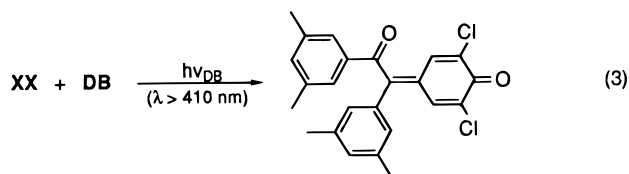
(iii) The unsymmetrical character of **DB** together with that of the acentric diarylacetylenes in Chart 1 presents a rigorous test for the regioselectivity in quinone methide formation.

Our task in this study is to first demonstrate that the direct photoexcitation of the carbonyl component (**DB**) leads to the Paterno–Büchi cycloadduct in eq 1, and that identical regioselectivities in the quinone methide result from the specific charge-transfer activation of the EDA complex. Time-resolved (ps, ns) spectroscopy will then define the temporal behavior of the ion-radical pairs as the prime reactive intermediates in the photocoupling processes.

Results

Photoactivations were carried out at a pair of wavelength regions, viz. (a) at $\lambda_{\text{exc}} > 410$ nm for the direct excitation of **DB** and (b) at $\lambda_{\text{exc}} > 530$ nm for the specific charge-transfer excitation of the electron donor–acceptor complexes of **DB** (vide infra).

I. Photoinduced Coupling of Diarylacetylenes by Direct Activation of 2,6-Dichlorobenzoquinone. An equimolar solution of the di-*m*-xylylacetylene **XX** and **DB** (0.01 M) in dichloromethane was first irradiated with visible light at $\lambda_{\text{exc}} > 410$ nm. Periodic GC analysis of the photosylate indicated the monotonic disappearance of both **XX** and **DB**, and the appearance of a single product. After 22 h, quantitative GC analysis revealed a 60% conversion of the reactants. The solvent was removed in vacuo, and the product isolated in 90% yield by flash chromatography. NMR and mass spectral analysis combined with elemental analysis confirmed the formation of a 1:1 adduct, and the structure of the adduct in eq 3 was established by X-ray crystallography (Figure 1).²⁴ There was no (NMR/GC) evidence for the formation of the isomeric product with the chlorine atoms located α - to the *exo*-methylene group.



The series of diarylacetylenes in Chart 1 were similarly irradiated together with **DB** at room temperature for 22 h, with the various conversions and yields reported in Table 1. In general, unsymmetrical diarylacetylenes generated only two of the four possible isomeric products. For example, the photolysis of an equimolar solution of phenyl-*m*-xylylacetylene **FX** and **DB** yielded a 10:1 ratio of two isomeric products. The regiochemistry of addition to the acetylene moiety was readily

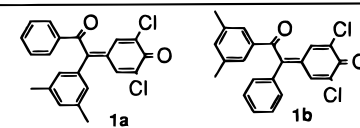
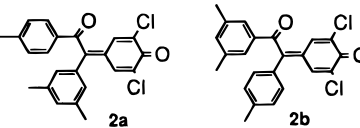
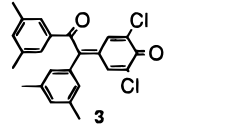
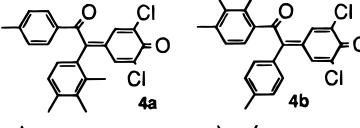
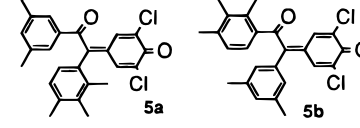
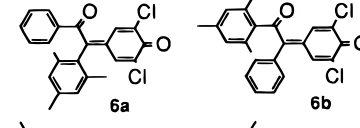
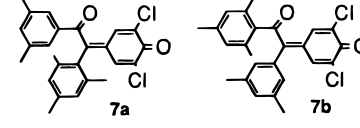
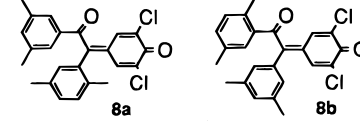
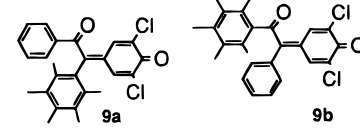
(21) The reduction potential (E_{red}) of triplet **DB** was estimated by using the equation $E_{\text{red}} = E_{\text{T}} + E^{\circ}_{\text{red}}$, where E_{T} is the triplet energy (ca. 2.2 eV)^{21a} and E°_{red} is the (ground-state) reduction potential (−0.18V vs SCE)^{21b} of dichlorobenzoquinone. See: (a) Murov, S. L.; Carmichael, I.; Hug, G. L. *Handbook of Photochemistry*, 2nd ed.; Dekker: New York, 1993; p 19. (b) Peover, M. E. *J. Chem. Soc.* **1962**, 4540.

(22) For photoinduced electron transfer involving quinones, see: (a) Mattay, J. *Angew. Chem., Int. Ed. Engl.* **1987**, *26*, 825 and references therein. (b) Mariano, P. S.; Stavinoha, J. L. In *Synthetic Organic Photochemistry*; Horspool, W. M., Ed.; Plenum Press: New York, 1984; p 145. (c) Bacocchi, E.; Del Giacco, T.; Elisei, F.; Ioele, M. *J. Org. Chem.* **1995**, *60*, 7974. (d) Pandey, G. In *Photoinduced Electron-Transfer V*; Mattay, J., Ed.; Springer-Verlag: New York, 1993; p 175. See also: Mattay, J. *Synthesis* **1989**, 233.

(23) Foster, R. *Organic Charge-Transfer Complexes*; Academic Press: New York, 1969; p 40.

(24) On deposit with the Cambridge Crystallographic Data Centre, University Chemical Laboratory, Lensfield Rd., Cambridge, CB2 1EW, U.K.

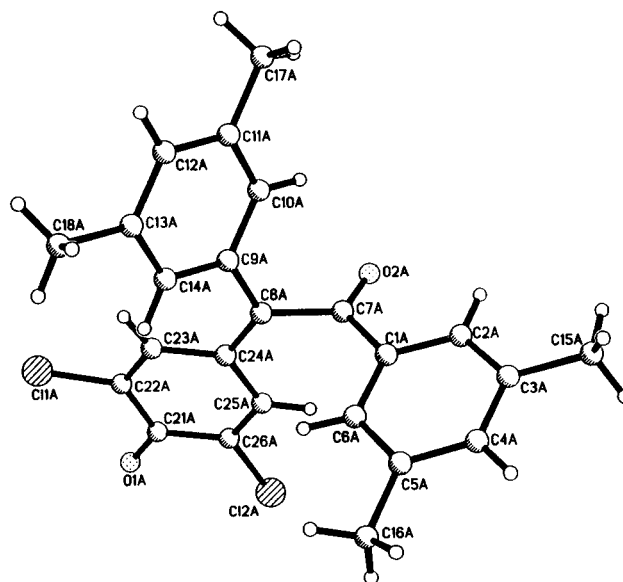
Table 1. Photoinduced Coupling of Diarylacetylene Donors and 2,6-Dichlorobenzoquinone^a

donor ^b	conv. ^{c,d} (%)	products	ratio ^d (a:b)	yield ^e (%)
FX	62		10:1	88
TX	58		3:2	82
XX	60		—	92
TH	35		25:1	90
XH	35		15:1	80
FM	30		25:1	90
XM	33		25:1	85
XX'	53		5:4	90
FP	26		25:1	85

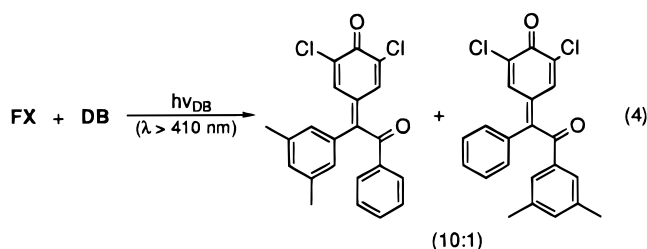
^a 0.1 M dichloromethane solutions irradiated at 25 °C with a medium pressure Hg lamp with a 410 nm cutoff filter for 47 h (see Experimental Section). ^b Identified in Chart 1. ^c Based on added donor. ^d Determined by quantitative GC using an internal standard. ^e Isolated yield based on recovered donor.

established by a rather straightforward analysis of the mass-spectral fragmentation pattern. In particular, the most abundant ion formed from the major isomer corresponded to the fragment C₆H₅CO by the ready cleavage of the benzoyl group,²⁵ and by contrast, the most abundant fragment of the minor product corresponded to the dimethylbenzoyl group (CH₃)₂C₆H₃CO to establish the methyl substitution pattern in both products. The proton NMR chemical shifts and coupling of the vinylic protons in the products were similar to those recorded for the single product from the symmetrical XX in eq 3. Thus, the regio-

(25) The favored MS fragmentation of benzoyl groups is described by: McLafferty, F. W.; Turecek, F. *Interpretation of Mass Spectra*, 4th ed.; University Science: Mill Valley, CA, 1993.

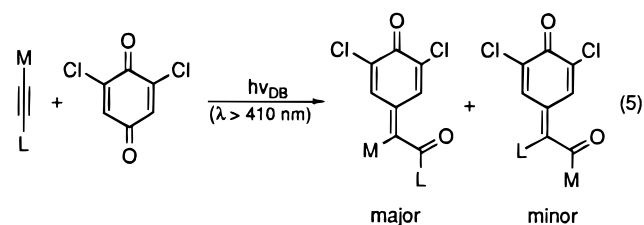
**Figure 1.** Molecular perspective of quinone methide **3** from the photoinduced coupling of di-*m*-xylylacetylene **XX** with dichloroquinone **DB**.

chemical disposition of the chloro groups was deduced as:



The regioselectivities in the other products in Table 1 were determined in a similar manner. The sole exception was the tetramethyl derivative **XX'**, in which both isomeric products (expectedly) displayed the same mass-spectral fragmentation pattern. Fortunately, the isomers separated themselves since the minor product spontaneously crystallized from the photolyzate when the photocoupling was performed in acetonitrile. Subsequent X-ray crystallographic analysis (see Figure 2 in the Supporting Information) established the substitution pattern of the adduct (Table 1).

It is particularly noteworthy that the additions to unsymmetrical acetylenes proceeded with remarkable selectivity to favor the most substituted benzylidene derivative and the least substituted benzoyl group (see generic representation in eq 5),



where M represents the more methylated phenyl group and L the less substituted group.

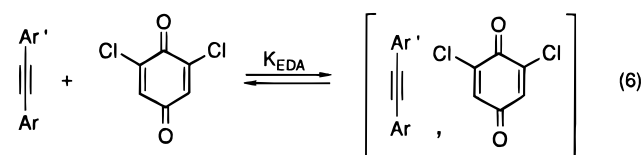
II. Characterization of the Electron Donor–Acceptor (EDA) Complexes of Diarylacetylenes with 2,6-Dichlorobenzoquinone. Intense orange to red colors were immediately apparent upon the addition of a diarylacetylene (colorless) to pale yellow solutions of **DB**. Furthermore, the colorations were

Table 2. Formation Constants of the Electron Donor–Acceptor (EDA) Complexes of Diarylacetylene Donors with 2,6-Dichlorobenzoquinone^a

donor	E_{ox} (V vs SCE) ^b	λ_{CT} (nm)	K_{EDA} (M ⁻¹)	ϵ_{CT} (M ⁻¹ cm ⁻¹)
FX	1.69	396	0.6	550
TX	1.61	428	0.4	900
XX	1.57	^c	0.9	800
TM	1.48	470	0.5	560

^a In dichloromethane solution at room temperature (see Experimental Section). ^b Peak potential of the irreversible anodic wave by CV at $v = 100$ mV s⁻¹ in dichloromethane solution containing 0.2 M Bu₄N⁺PF₆⁻ electrolyte. ^c Spectral subtraction did not yield a distinct maximum.

clearly related to the extent of methyl substitution—the dimethyl derivatives forming yellow solutions—but successive methyl substitutions resulted in progressively darker red hues. These colored solutions persisted indefinitely provided they were stored in the dark. Most importantly, the component quinones and acetylenes could be quantitatively recovered intact from mixtures that were even stored for several days at room temperature (in the dark). The coloration was however subject to successive enhancement upon incremental additions of diarylacetylene, as shown by the series of UV–vis spectral changes in Figure 3 (see Supporting Information), which typified the formation of electron donor–acceptor (EDA) complexes in solutions,^{23,26} e.g.



Consequently, the spectral change was quantitatively monitored at the absorption maximum by using the Benesi–Hildebrand relationship,²⁷ i.e.

$$\frac{[DB]}{A_{CT}} = \frac{1}{K_{EDA} \epsilon_{CT} [DA]} + \frac{1}{\epsilon_{CT}} \quad (7)$$

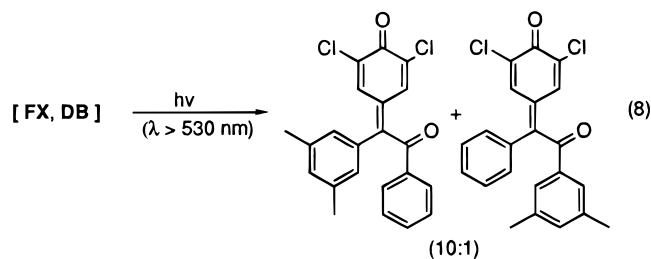
where K_{EDA} represents the formation constant and ϵ_{CT} the extinction coefficient of the EDA complex. The values of K_{EDA} and ϵ_{CT} obtained from this relationship are listed in Table 2 along with the absorption maxima of the EDA complex. The absorption maxima listed in Table 2 were determined by the digital subtraction (shown in the inset to Figure 3 in the Supporting Information) of the absorbances due to the uncomplexed acetylenes and the quinone from the absorption band of the mixture. The relationship between the absorption maximum and the extent of methyl substitution was further quantified by evaluating the donor strength of the various diarylacetylenes as given by their irreversible oxidation potentials (E_{ox} in V vs SCE).²⁸ Indeed, the progressive red shift of the absorption band was directly correlated with the donor strength of the acetylenes (Table 2) to establish the charge-transfer character of the EDA complex in eq 6, as described by Mulliken.²⁹

Slow removal of the solvent from the dichloromethane solution of tolyl-*m*-xylylacetylene **TX** and **DB** (at 20 °C in the

dark) yielded orange needles, GC and NMR analysis of which indicated a 2:1 molar mixture of **DB** and **TX**. The same stoichiometry was obtained for other orange crystals, irrespective of the molar ratio (varied from 1:2 to 4:1) of the components extant in the solution from which they were derived. X-ray crystallographic analysis of a single orange crystal showed it to consist of stacks of alternate donor (**TX**) and acceptor (**2DB**) molecules. The face-to-face π -complexation (of each quinone with both aromatic moieties of **TX**) that identifies the charge-transfer interaction in the EDA complex is depicted in Figure 4.³⁰

Single crystals of the EDA complex were also readily obtained from solutions of the diarylacetylenes **FP**, **XM**, **XH**, and **XX** with the quinone acceptor **DB**; and in all cases a consistent 2:1 molar composition was obtained. The X-ray crystallography of the colored charge-transfer crystals from **FP** and **XX** with **DB** showed that similar donor–acceptor stacks were formed with the parallel cofacial orientation of the quinone relative to the long axis of the acetylene.³¹ The colors of the charge-transfer crystals were comparable to the colored solutions of the same components in dichloromethane (Table 2), i.e. dark red crystals were obtained from **FP** and **DB**, whereas orange crystals were obtained from **FX** and **DB**.

III. Charge-Transfer Photocoupling of Diarylacetylenes and 2,6-Dichlorobenzoquinone. The distinct charge-transfer absorption bands associated with the EDA complexes in solution (see Figure 3 in the Supporting Information) permitted their specific photoexcitation by actinic irradiation at $\lambda_{exc} > 530$ nm. Under these conditions, any adventitious excitation of either the uncomplexed **DB** or diarylacetylene was clearly precluded. Accordingly, equimolar solutions of **FX** and **DB** (0.1 M) were next irradiated with visible light from a medium pressure (500-W) mercury lamp fitted with a sharp cutoff filter with $\lambda_{exc} > 530$ nm. Periodic GC analysis of the photosylate indicated the steady formation of 1:1 adducts; and the final analysis of the reaction mixture by quantitative GC after 47 h indicated a ~10% conversion of the reactants to a 10:1 mixture of two isomeric adducts:



which was the same as that obtained by direct excitation of **DB** (at $\lambda_{exc} > 410$ nm) in the presence of **FX**, as described in Table 1. Furthermore, the charge-transfer activation of the other diarylacetylene/**DB** complexes afforded analogous pairs of 1:1 adducts, but with the different conversions and yields listed in Table 3. Further differences in the efficiency of the direct and charge-transfer excitation were investigated by evaluating the quantum yields for photolysis at $\lambda_{exc} > 410$ nm compared to that at $\lambda_{exc} > 530$ nm.

IV. Quantum Efficiencies for the Direct and Charge-Transfer Photocoupling of Diarylacetylenes and 2,6-Dichlorobenzoquinone. The quantum efficiencies for photocouplings

(26) (a) Briegleb, G. *Elektronen Donator–Acceptor Komplexe*; Springer: Berlin, 1961. (b) Andrews, L. J.; Keefer, R. M. *Molecular Complexes in Organic Chemistry*; Holden-Day: San Francisco, 1964.

(27) (a) Benesi, H. A.; Hildebrand, J. H. *J. Am. Chem. Soc.* **1949**, *71*, 2703. (b) Person, W. B. *J. Am. Chem. Soc.* **1965**, *87*, 167.

(28) For the cyclic voltammetry, see Experimental Section.

(29) (a) Mulliken, R. S. *J. Am. Chem. Soc.* **1950**, *72*, 600. (b) Mulliken, R. S. *J. Am. Chem. Soc.* **1952**, *74*, 811. (c) Mulliken, R. S. *J. Phys. Chem.* **1952**, *56*, 801. (d) Mulliken, R. S.; Person, W. M. *Molecular Complexes*; Wiley: New York, 1969.

(30) Compare: Harding, T. T.; Wallwork, S. C. *Acta Crystallogr.* **1955**, *8*, 787.

(31) Bosch, E.; Hubig, S. M.; Lindeman, S. V.; Kochi, J. K. *J. Org. Chem.* In press.

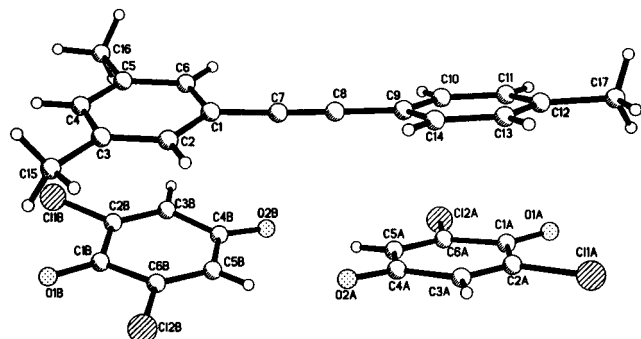
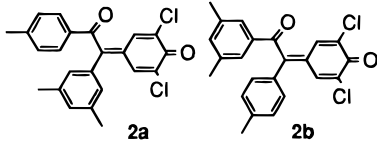
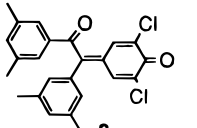
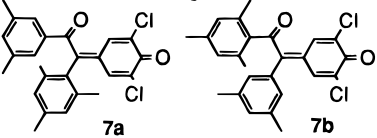
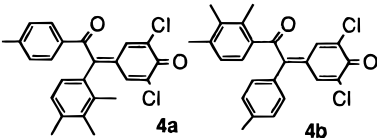


Figure 4. Molecular structure of the EDA complex of tolyl-*m*-xylylacetylene (**TX**) and **DB**, showing the cofacial donor–acceptor interactions.

Table 3. Charge-Transfer Photocoupling of Diarylacetylenes and 2,6-Dichlorobenzoquinone^a

donor	conv. ^{b,c} (%)	products	ratio ^c	yield ^d (%)
TX	8		3:2	85
XX	15		-	90
XM	8		25:1	85
TH	10		25:1	88

^a 0.1 M dichloromethane solutions irradiated at 25 °C with a medium pressure Hg lamp with a 530 nm cutoff filter for 47 h (see Experimental Section). ^b Based on added donor. ^c Determined by quantitative GC using an internal standard. ^d Isolated yield based on recovered donor.

at the two wavelength regions (represented by the results in Tables 1 and 3) were evaluated by (a) ferrioxalate actinometry³² with monochromatic light at $\lambda_{\text{exc}} = 440$ nm and (b) Reineckate salt actinometry³³ at $\lambda_{\text{exc}} = 580$ nm, as described in the Experimental Section. The representative results in Table 4 clearly showed that the specific excitation of the charge-transfer absorption bands was a rather inefficient process with quantum efficiencies in the neighborhood of 0.1%. By contrast, the direct excitation of **DB** at 440 nm led to a more efficient photocoupling with $\Phi \approx 0.1$ (i.e. 10%) in Table 4, column 2.

V. Time-Resolved Spectroscopy of the Reactive Intermediates in the Photoinduced Coupling of Diarylacetylenes and Dichlorobenzoquinone. The reactive intermediates in the

(32) Hatchard, C. G.; Parker, C. A. *Proc. R. Soc.* **1956**, 235A, 518. See also: Calvert, J. G.; Pitts, J. N., Jr. *Photochemistry*; Wiley: New York, 1966; p 786.

(33) Wegner, E. E.; Adamson, A. W. *J. Am. Chem. Soc.* **1966**, 88, 394. See also: Bunce, N. J. In *Handbook of Organic Photochemistry*; Scaiano, J. C., Ed.; CRC Press: Boca Raton, FL, 1989; Vol. 1, Chapter 9, p 241ff.

Table 4. Quantum Yields for the Direct- and Charge-Transfer Photocoupling of Diarylacetylene Donors with 2,6-Dichlorobenzoquinone^a

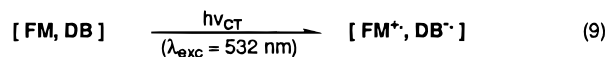
donor	quantum yield	
	at $\lambda_{\text{DB}} = 440$ nm ^b	at $\lambda_{\text{CT}} = 580$ nm ^c
FX	0.11	1.0×10^{-3}
TX	0.09	0.8×10^{-3}
XX	0.10	
XH	0.05	
XM		1.1×10^{-3}
FP	0.03	
FM	0.08	

^a In dichloromethane solution at room temperature (see Experimental Section). ^b Determined by ferrioxalate actinometry^b or Reineckate salt actinometry^c (see Experimental Section).

direct and charge-transfer photocoupling processes in Tables 1 and 3 were interrogated by time-resolved spectroscopy in two separate time domains, as follows.³⁴

A. Charge-Transfer Excitation of the Ground-State EDA Complex of 2,6-Dichlorobenzoquinone and Diarylacetylene.

The ground-state EDA complex in eq 6 was subject to specific (vertical) excitation by deliberate irradiation of its charge-transfer absorption band.³⁵ Thus, the laser pulse at $\lambda_{\text{exc}} = 532$ nm corresponding to the second harmonic of a mode-locked Nd³⁺:YAG laser³⁴ was well suited for the specific excitation of the charge-transfer bands derived from the diarylacetylenes and **DB** in Table 2. The time-resolved (ps) absorption spectrum observed upon the application of a 25-ps (fwhm) laser pulse at $\lambda_{\text{exc}} = 532$ nm to a solution of 0.11 M **FM** and 0.05 M **DB** in dichloromethane is shown in Figure 5A consisting of a somewhat narrow band at $\lambda_{\text{max}} = 435$ nm and a pair of broader bands centered at 600 and 800 nm. The principal spectral features in Figure 5A coincided with the absorption spectrum shown in Figure 5B of the phenyl(mesityl)acetylene cation radical (**FM**^{•+}), which was independently generated.³⁶ However, a close (comparative) inspection of the spectra in Figures 5A and 5B suggested the presence of a low-energy tail on the 435-nm band in Figure 5A. Indeed, spectral subtraction of the **FM**^{•+} spectrum (Figure 5B) from the experimental spectrum (Figure 5A) resulted in a well-resolved absorption band with $\lambda_{\text{max}} = 450$ nm (see inset, Figure 5A), which corresponded to the absorption spectrum of dichlorobenzoquinone anion radical (**DB**^{•-}). The latter was verified by direct spectral comparison with **DB**^{•-} generated independently.³⁷ We judge from the relative spectral intensities of **FM**^{•+} and **DB**^{•-} in Figure 5A that this cation-radical/anion-radical pair was formed in a roughly 1:1 molar ratio,³⁸ i.e.



The composite spectrum in Figure 5A decayed (at all wave-

(34) See: Bockman, T. M.; Kochi, J. K. *J. Chem. Soc., Perkin Trans. 2*, **1996**, 1633.

(35) Kochi, J. K. *Acta Chem. Scand.* **1990**, 44, 409.

(36) The authentic spectrum of **FM**^{•+} was obtained by charge-transfer excitation of the EDA complex of **FM** with maleic anhydride in dichloromethane. Note that the anion radical of maleic anhydride does not absorb in the detection window between 400 and 800 nm.

(37) The authentic spectrum of **DB**^{•-} was obtained by electron-transfer quenching of the photoexcited (triplet) **DB** with dibenzofuran donor in acetonitrile. Note that the cation radical of the donor does not absorb in the 400 to 500 nm region.

(38) By taking the extinction coefficient of **DB**^{•-} at 450 nm to be $\epsilon = 6800 \text{ M}^{-1} \text{ cm}^{-1}$ and that of **FM**^{•+} at 600 nm to be $\epsilon = 3500 \text{ M}^{-1} \text{ cm}^{-1}$, as described by: Rathore, R.; Hubig, S. M.; Kochi, J. K. *J. Am. Chem. Soc.* **1997**, 119, 11468. Shida, T. *Electronic Absorption Spectra of Radical Ions*; Elsevier: New York, 1988.

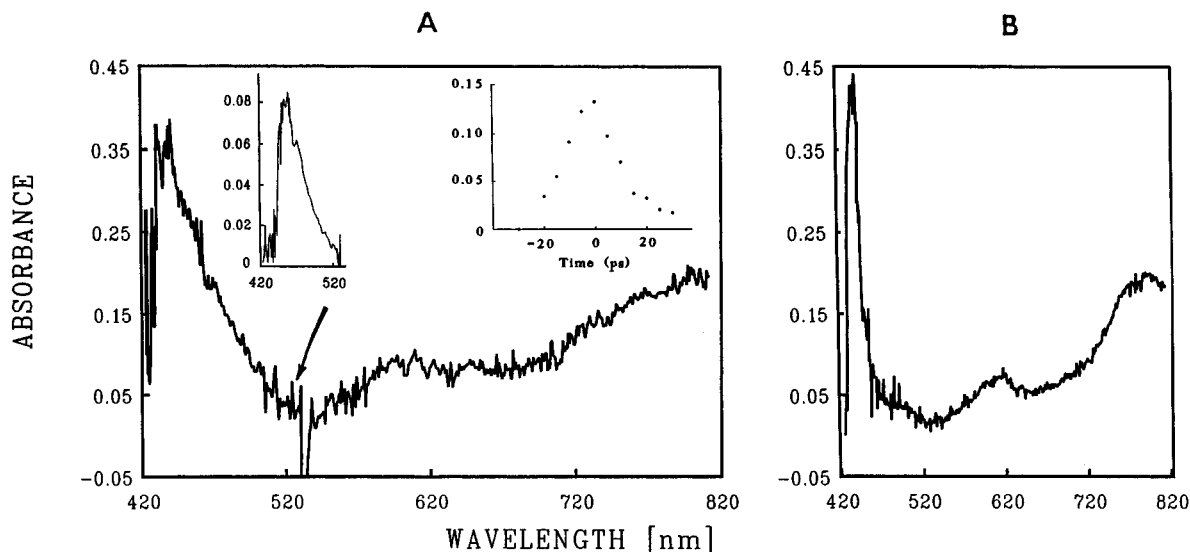


Figure 5. (A) Transient (ps) spectrum obtained from the application of a 25-ps laser pulse at $\lambda_{CT} = 532$ nm to a solution of 0.11 M phenyl(mesityl)acetylene (**FM**) and 0.05 M dichlorobenzoquinone (**DB**) in dichloromethane. Inset: (Left) Difference spectrum of the anion radical **DB** $^{\bullet-}$ obtained by digital subtraction of the authentic spectrum of **FM** $^{\bullet+}$ shown in part B.^{36,37} (Right) Temporal evolution of **FM** $^{\bullet+}$ in the time interval from 0 to 35 ps.

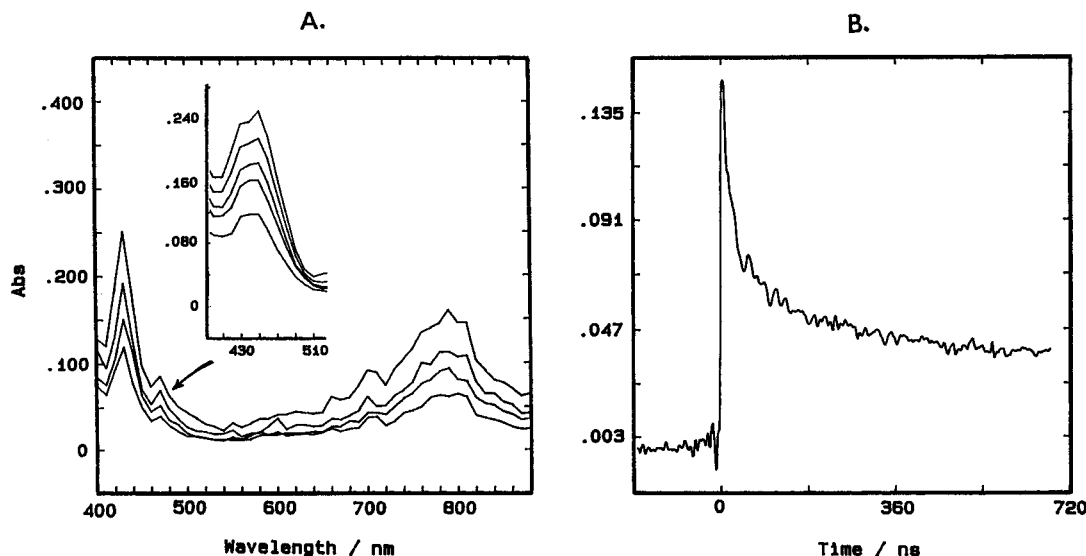
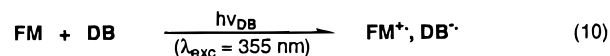


Figure 6. (A) Transient spectra obtained from the application of a 10-ns laser pulse at $\lambda_{DB} = 355$ nm to a solution of 0.10 M phenyl(mesityl)acetylene (**FM**) and 0.01 M dichlorobenzoquinone (**DB**) in dichloromethane. Inset: Absorption spectrum of authentic dichloroquinone anion radical (**DB** $^{\bullet-}$), as described in the text. (B) Biphasic decay of the **FM** $^{\bullet+}$ transient showing initial first-order kinetics (k_1) to $\sim 30\%$ residual, followed by second-order decay to the microsecond time domain (not shown).

lengths in the spectral region from 420 to 800 nm) to the spectral baseline within the 25-ps time period of the laser excitation (see Figure 5A inset), from which we estimate $k_{decay} \geq 4 \times 10^{10} \text{ s}^{-1}$.

B. Direct Excitation of 2,6-Dichlorobenzoquinone in the Presence of Diarylacetylenes. To probe the nature of the intermediates formed upon the direct excitation of the quinone (corresponding to the preparative results in Table 1 from irradiation with light of $\lambda_{exc} > 410$ nm), a solution of **DB** in the presence of phenyl(mesityl)acetylene **FM** in dichloromethane was subjected to a 10-ns excitation pulse from a Q-switched Nd $^{3+}$:YAG laser at 355 nm.^{34,39} The time-resolved (ns) absorption spectrum in Figure 6A closely resembled the (ps) spectrum obtained from the charge-transfer excitation in Figure 5A. Accordingly, the transient spectrum was analyzed as a composite spectrum resulting from a 1:1 molar mixture of

FM $^{\bullet+}$ and **DB** $^{\bullet-}$ (see inset),^{36,37} i.e.



The (ns) spectrum in Figure 6A decayed uniformly (in the spectral region from 400 and 850 nm) to a raised spectral

(39) (a) It needs to be re-emphasized that the observation of ion radicals upon direct excitation of the quinone is of mechanistic relevance only when combined with the unambiguous observation of ion radicals upon charge-transfer excitation. (b) Although the "local" band of **DB** and the CT band of the EDA complex overlap at 355 nm, the laser pulse effectively excited **DB** under the conditions employed in Table 1 owing to the very low concentrations of the EDA complex due to the limited values of K_{EDA} in Table 2. (c) Excitation of **DB** was carried out at the red-shifted region of $\lambda_{exc} > 410$ nm for the preparative studies to minimize complications from the steadily increasing concentrations of the bright yellow (quinone methide) products with $\lambda_{max} \approx 400$ nm.

baseline on the ns/ μ s time scale with biphasic kinetics (Figure 6B) consisting of a fast first-order decay with $k_1 = 5.5 \times 10^7 \text{ s}^{-1}$ followed by a slower second-order decay with $k_2 \approx 10^{10} \text{ M}^{-1} \text{ s}^{-1}$ (vide infra). The ratio of the fast and slow components was estimated to be $\sim 2:1$.

Discussion

I. Reactivity Patterns in the Photoactivated Coupling of Diarylacetylenes and Quinone. Photoinduced couplings of the diarylacetylenes in Chart 1 with the prototypical quinone acceptor **DB** (as presented in Tables 1 and 3) show a number of unusual but characteristic reactivity patterns such as the following: (A) the coupled products are formed in high yields with regioselectivities that *strongly* favor only one isomer, particularly from those diarylacetylenes containing different numbers of methyl substituents on the aromatic rings, and the preponderant isomer always contains the less methylated benzoyl group; (B) additions to the dichlorobenzoquinone moiety occur regiospecifically at the oxygen center further removed from the 2,6-dichloro groups so that only two of the four possible isomers are always formed; (C) electron donor–acceptor (EDA) complexes are spontaneously formed according to the reversible preequilibrium in eq 6, and they show diagnostic charge-transfer absorption bands in the visible (spectral) region in Table 2; and (D) the compositions of the isomeric mixture of the coupling products are singularly unaffected by the actinic (energy) input at either $\lambda_{\text{exc}} > 410 \text{ nm}$ (70 kcal mol^{-1}) or $\lambda_{\text{exc}} > 530 \text{ nm}$ (54 kcal mol^{-1}).

II. Photoinduced Electron Transfers between Quinone and Diarylacetylenes. Any mechanistic formulation must take into account all of the diverse facets of the photoinduced couplings of quinones with diarylacetylenes as described in A–D above. Accordingly, let us first consider what time-resolved spectroscopy tells us about the reactive intermediates responsible for such a unique reactivity pattern. Figures 5 and 6 both indicate that the ion-radical pair $^1[\text{FM}^+, \text{DB}^{\cdot-}]$ is the first (discernible) species from the oxidized phenyl(mesityl)acetylene donor **FM** and the reduced dichloroquinone acceptor **DB**. Such a commonality of reactive intermediates exists irrespective of the photoexcitation wavelength and the time scale of the spectroscopic observation—the spectral decay of $k_1 \sim 6 \times 10^7 \text{ s}^{-1}$ in Figure 6B being 3 orders of magnitude slower than the (ps) decay in Figure 5A (inset) with $k_1 \geq 4 \times 10^{10} \text{ s}^{-1}$. Nonetheless, both pairs of ion radicals lead to the common set of coupled products with the identical (relative) yields shown in Tables 1 and 3. Accordingly, let us consider separately the two photoactivation processes in the following way.

Photoactivation of the EDA complex by irradiation of the charge-transfer absorption band with a 25-ps laser pulse at $\lambda_{\text{exc}} = 532 \text{ nm}$ results in the spontaneous electron transfer from the acetylene donor to the quinone acceptor,⁴⁰ as described above in eq 9. Consequently, the resulting singlet ion-radical pair⁴¹ in Figure 5 represents unambiguously the first reactive intermediate that must lead to coupling (k_c) to form the adduct **FM-DB**. However, the ion-radical pair also reacts by back electron

transfer (k_{BET}) that regenerates the starting materials **FM** and **DB**. The overall result is the (first-order) competition between coupling and back electron transfer to be described as:

Scheme 1



In fact, we conclude from the low photochemical efficiency of coupling (Table 4) with $\Phi_{\text{CT}} \approx 1 \times 10^{-3}$ that the fast decay of the ion-radical pair to the spectral baseline in Figure 5A is almost entirely due to back electron transfer. As such, we reckon from Scheme 1 that $\Phi_{\text{CT}} = k_c/(k_{\text{BET}} + k_c)$, and coupling proceeds via the rather diminished rate constant of $k_c = 4 \times 10^7 \text{ s}^{-1}$. In other words, photoinduced coupling via the charge-transfer excitation of the EDA complex $[\text{FM}, \text{DB}]$ is a rather inefficient process due to the high efficiency of the energy-wasting back electron transfer, as given by the factor of 10^3 that separates k_{BET} and k_c in Scheme 1. Indeed, such a kinetics behavior of $^1[\text{FM}^+, \text{DB}^{\cdot-}]$ derived from the specific charge-transfer excitation has been observed previously for various types of other EDA complexes,⁴² and it can be used to define $^1[\text{FM}^+, \text{DB}^{\cdot-}]$ in Scheme 1 as the contact ion-radical pair.⁴⁰

Direct activation of the quinone acceptor by irradiation of **DB** with a 10-ns laser pulse at $\lambda_{\text{exc}} = 355 \text{ nm}$ also results in electron transfer from the acetylene donor to the quinone acceptor, as described in eq 10. We judge from the biphasic decay in Figure 6B that the pair of ion radicals FM^+ and $\text{DB}^{\cdot-}$ exist in two kinetically distinguishable forms, i.e. as ion-radical pairs $[\text{FM}^+, \text{DB}^{\cdot-}]$ which are rather short-lived and as “free” solvated ions (FM^+ and $\text{DB}^{\cdot-}$) which react at slower rates controlled by diffusion.

Based on the rapid coproduction of FM^+ and $\text{DB}^{\cdot-}$ within 10 ns of the laser excitation (Figure 6), we conclude that the initial electron transfer occurs with a bimolecular rate constant of $k_{\text{ET}} = k_{\text{obs}}/[\text{FM}] \geq 10^9 \text{ M}^{-1} \text{ s}^{-1}$, which is close to that of diffusion-controlled processes.⁴³ Indeed, previous studies have shown that the application of a laser pulse at $\lambda_{\text{exc}} = 355 \text{ nm}$ to chloranil and related quinone acceptors leads to their efficient excitation to the triplet state Q^* ^{19,39b} with a sizable energy of $E_T \approx 50 \text{ kcal mol}^{-1}$,^{19,44} which is sufficient to effect diffusional quenching by electron transfer from aromatic donors of the type in Chart 1, to afford the triplet ion-radical pair,⁴⁵ i.e.

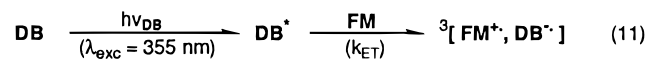


Figure 6B shows that the triplet ion-radical pair $^3[\text{FM}^+, \text{DB}^{\cdot-}]$ in eq 11 decays within 18 ns to $\sim 30\%$ of its initial absorbance with rate constant $k_1 = 5.5 \times 10^7 \text{ s}^{-1}$. The residual absorption then decays slowly by second-order kinetics over a period of nanoseconds and extending into the microsecond domain (not shown); and it is thus ascribed to the “free” solvated ions FM^+

(40) (a) Peters, K. S.; Li, B. *J. Phys. Chem.* **1994**, *98*, 401. (b) Peters, K. S. In *Advances in Electron-Transfer Chemistry*; JAI Press: New York, 1994; Vol. 4, p 27. (c) Asahi, T.; Mataga, N. *J. Phys. Chem.* **1989**, *93*, 6575. (d) Asahi, T.; Mataga, N. *J. Phys. Chem.* **1991**, *95*, 1956. (e) Hubig, S. M.; Bockman, T. M.; Kochi, J. K. *J. Am. Chem. Soc.* **1996**, *118*, 3842. (f) Hilinski, E. F.; Masnovi, J. M.; Kochi, J. K.; Rentzepis, P. M. *J. Am. Chem. Soc.* **1984**, *106*, 8071.

(41) Direct photoactivation of the EDA complex produces the singlet ion pair in eq 9 and Scheme 1. See: (a) Ojima, S.; Miyasaka, H.; Mataga, N. *J. Phys. Chem.* **1990**, *94*, 4147. (b) Wynne, K.; Galli, C.; Hochstrasser, R. M. *J. Chem. Phys.* **1994**, *100*, 4797.

(42) For other examples of the competition between back electron transfer (k_{BET}) and various other irreversible chemical processes (k_c) stemming from the ion-radical pair, see: (a) Wallis, J. M.; Kochi, J. K. *J. Am. Chem. Soc.* **1988**, *110*, 8207. (b) Bockman, T. M.; Hubig, S. M.; Kochi, J. K. *J. Org. Chem.* **1997**, *62*, 2210. (c) Masnovi, J. M.; Kochi, J. K.; Hilinski, E. F.; Rentzepis, P. M. *J. Am. Chem. Soc.* **1986**, *108*, 1126. (d) Bockman, T. M.; Lee, K. Y.; Kochi, J. K. *J. Chem. Soc., Perkin Trans. 2* **1992**, 1581. (e) Bockman, T. M.; Kochi, J. K. *J. Chem. Soc., Perkin Trans. 2* **1996**, 1633.

(43) We were unable to find (spectroscopic) evidence for the presence of 1,4-biradicals prior to ion-radical formation on the picosecond time scale as previously observed by Peters et al. for benzophenone in ref 15.

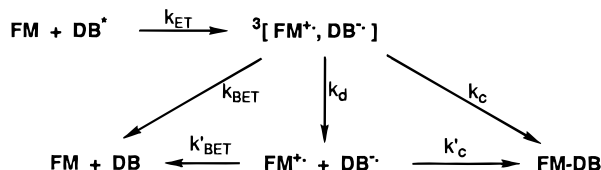
(44) Murov, S. L.; Carmichael, I.; Hug, G. L. *Handbook of Photochemistry*, 2nd ed.; Dekker: New York, 1993.

(45) Diffusional quenching of the excited quinone DB^* results in the formation of the triplet ion pair in eq 11.⁴⁶

and $\text{DB}^{\cdot-}$. The recombination of these solvated ion radicals on the ns/ μs time scale occurs with a bimolecular rate constant of $k_2 \approx 10^{10} \text{ M}^{-1} \text{ s}^{-1}$.

From a consideration of the microdynamical processes extant in Scheme 2, we suggest that the initial decay ($k_1 = 5.5 \times 10^7 \text{ s}^{-1}$) reflects the competition among three first-order rate processes, i.e. $k_1 = k_d + k_{\text{BET}} + k_c$, as schematically presented below.

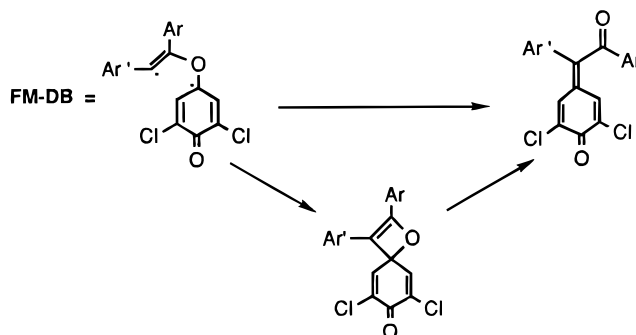
Scheme 2



The rate constant for the dissociation of the ion pair (leading to the free ions) in Scheme 2 can be calculated as $k_d = \Phi_{\text{ions}} k_1 = 1.7 \times 10^7 \text{ s}^{-1}$, based on the yield of free ions of $\Phi_{\text{ions}} = 0.3$ (which corresponds to the 30% residual absorbance observed after 18 ns, vide supra). Thus, the sum of back electron transfer and coupling amounts to $k_{\text{BET}} + k_c = 3.8 \times 10^7 \text{ s}^{-1}$. Since the overall quantum yield for the coupling products in Table 4 ($\Phi_{\text{ions}} \approx 0.1$ in column 2) points to a rate-constant ratio of $k_c/(k_c + k_{\text{BET}}) = 0.1$,⁴⁷ we calculate the back electron-transfer rate as $k_{\text{BET}} = 3.4 \times 10^7 \text{ s}^{-1}$ and the coupling rate as $k_c = 4 \times 10^6 \text{ s}^{-1}$.⁴⁸ Finally, we ascribe the slow decay of the free ion radicals on the ns/ μs time scale to a combination of back electron-transfer (k'_{BET}) and coupling (k'_c), the branching ratio of which is expected to be the same as that in the first-order processes, i.e. $k'_c/(k'_c + k'_{\text{BET}}) \sim 0.1$.

III. Formation of Photocoupling Products. The time-resolved (ps and ns) spectra in Figures 5 and 6 establish the ion radicals from diarylacetylenes and dichlorobenzoquinone as the reactive intermediates. In the case of the specific charge-transfer excitation of the [FM, DB] complex, the ion-radical pair is the direct precursor to the coupling products. Since we obtain the same coupling products with their unique regioselectivities independent of the irradiation wavelength (λ_{CT} or λ_{DB}), we conclude that direct photoactivation of the quinone leads to the same sequence of steps, i.e. formation of the ion-radical pair followed by coupling. Thus, the collapse of the ion-radical pair to the distonic acetylene/quinone adduct FM-DB is common to both the charge-transfer and the direct photoactivations in Schemes 1 and 2, respectively. Since the subsequent transformation of this intermediate is not revealed by the time-resolved spectroscopic studies,^{47b} the pathway to the photocoupling products in Tables 1 and 3 can only be inferred from the structures of the quinone methides (such as in Figure 1). Accordingly, we can envisage at least two routes that proceed from the ion-pair adduct to the quinone methide, as illustrated

Scheme 3



in Scheme 3. Simple cyclization of the distonic biradical leads to the labile oxetene previously reported by Friedrich and co-workers.¹¹ This pathway is also reasonable on the basis of the photocoupling of benzoquinones with stilbenes to afford stable oxetanes.^{49,50} [Furthermore, the initial formation of a biradical as a result of ion-pair collapse relates to an analogous intermediate in the formation of oxetanes from benzoquinone and olefins.⁵¹] Conceptually, the same transformation to the quinone methide may occur in a single step by a concerted electrocyclic rearrangement of the distonic biradical. Be that as it may, the ion-pair collapse to the distonic biradical in the step (k_c) largely determines the regioselectivities observed in Tables 1 and 3. Since organic cation radicals are known to possess electrophilic reactivity,^{52,53} we envisage the ion-pair collapse as a nucleophilic attack of the quinone anion radical at the cationic acetylenic center. [Neither quinone anion radicals nor diarylacetylene cation radicals show much homolytic reactivity,⁵⁴ and the alternative formation of a zwitterionic adduct is disfavored.] If so, the regioselectivity of the quinone moiety derives from a negative charge that is more localized on the distal oxygen of DB as a result of the electron-withdrawing properties of the 2,6-dichloro substituents. The regioselectivity in the diarylacetylene moiety is more difficult to rationalize. However, the preponderant formation of the quinone methide with the less methylated benzoyl group is consistent with nucleophilic attack of the less hindered oxyanion occurring on the diarylacetylene cation radical at the less hindered acetylene carbon center.⁵⁵

Summary and Conclusions

The photoaddition of the quinone DB onto diarylacetylene to afford the quinone methides in Tables 1 and 3 is effectively

(49) Xu, J.-H.; Wang, L.-C.; Xu, J.-W.; Yan, B.-Z.; Yuan, H.-C. *J. Chem. Soc., Perkin Trans. 1* **1994**, 571 and references therein.

(50) See also: Bryce-Smith in ref 8b.

(51) Similar biradicals have been trapped with dioxygen during the irradiation of *p*-benzoquinone in the presence of styrene: Wilson, R. M.; Wunderly, S. W.; Walsh, T. F.; Musser, A. K.; Outcalt, R.; Geiser, F.; Gee, S. K.; Brabender, W.; Yerino, L., Jr.; Conrad, T. T.; Tharp, G. A. *J. Am. Chem. Soc.* **1982**, *104*, 4429.

(52) (a) Workentin, M. S.; Johnston, L. J.; Wayner, D. D. M.; Parker, V. D. *J. Am. Chem. Soc.* **1994**, *116*, 8279. (b) Norrsell, F.; Handoo, K. L.; Parker, V. D. *J. Org. Chem.* **1993**, *58*, 4929.

(53) (a) Evans, J. F.; Blount, H. N. *J. Org. Chem.* **1976**, *41*, 516. (b) Johnston, L. J.; Schepp, N. P. *J. Am. Chem. Soc.* **1993**, *115*, 6564.

(54) For a discussion of zwitterion versus biradical formation as a result of ion-radical coupling, see: Hall, H. K., Jr.; Padias, A. B. *Acc. Chem. Res.* **1990**, *23*, 3; **1997**, *30*, 322.

(55) Such a high selectivity of diarylacetylene cation radicals toward nucleophiles is analogous to that shown by related cation radicals derived from electron-rich (aryl)olefins, etc. See: (a) Johnston, L. J.; Schepp, N. P. In *Advances in Electron-Transfer Chemistry*; JAI Press: New York, 1996; Vol. 5, p 41. (b) Schepp, N. P.; Johnston, L. J. *J. Am. Chem. Soc.* **1994**, *116*, 10330. (c) Schepp, N. P.; Johnston, L. J. *J. Am. Chem. Soc.* **1996**, *118*, 2872. (d) Bauld, N. L. In *Advances in Electron-Transfer Chemistry*; JAI Press: New York, 1992; Vol 2, p 1. (e) See also: Xu et al. in refs 8 and 49.

(46) (a) Gschwind, R.; Haselbach, E. *Helv. Chim. Acta* **1979**, *62*, 941. (b) Johnston, L. J.; Schepp, N. P. *J. Am. Chem. Soc.* **1993**, *115*, 6564. (c) Levin, P. P.; Kuz'min, V. A. *Russ. Chem. Rev.* **1987**, *56*, 307. (d) Kobashi, H.; Funabashi, M.-A.; Kondo, T.; Morita, T.; Okada, T.; Mataga, N. *Bull. Chem. Soc. Jpn.* **1984**, *57*, 3557.

(47) (a) The coupling step (k_c) is considered to be rate-determining in the formation of the photoproducts. (b) The coupling step leading to the formation of quinone methide could not be observed directly in the laser experiments due to the low quantum yields (<0.1 , see Table 4) of this process. Thus, any weak absorptions of the quinone methides would be obscured by the strong absorption of the quinone anion radical ($\text{DB}^{\cdot-}$), which absorbs in the same wavelength region (400–500 nm).

(48) Values of k_{BET} and k_c for CT activation that are different from those by direct activation largely reflect the difference of the lifetimes of the singlet ion pair $^1[\text{FM}^+, \text{DB}^{\cdot-}]$ and the triplet ion pair $^3[\text{FM}^+, \text{DB}^{\cdot-}]$ in Schemes 1 and 2, respectively.

initiated by either (a) direct excitation of the quinone or (b) specific CT activation of the preequilibrium EDA complex of the quinone and acetylene (see Table 2). Time-resolved spectroscopy following laser-flash excitation establishes ion-radical pairs (consisting of quinone anion radicals and diarylacetylene cation radicals) to be the prime reactive intermediates in both actinic processes. The high regioselectivity to yield essentially one of the four possible isomeric quinone methides is attributed to the ion-radical pair collapse to afford the distonic biradical in Scheme 3. The competition from back electron transfer (k_{BET}) as described in Schemes 1 and 2 is responsible for limiting the efficacy of the product-determining coupling step (k_{C}) and the quantum yields in Table 4. In a more general context, the striking observation of identical photoproducts with the unique regioselectivities in Tables 1 and 3 provides compelling evidence that the Paterno–Büchi coupling of diarylacetylenes with quinone (via direct excitation of **DB**) evolves from the same sequence of reactive intermediates established by the charge-transfer activation, viz. initial electron transfer leads to ion-radical pairs, followed by coupling to the distonic biradical, oxetene formation and rearrangement to the quinone methides.⁵⁶ The applicability of such a mechanistic pathway to other unsaturated donors and carbonyl acceptors is presently under investigation.

Experimental Section

Materials. Phenylacetylene, 4-ethynyltoluene, mesitylene, pentamethylbenzene, 1,2,3-tri-methylbenzene, (trimethylsilyl)acetylene, 2,6-dichloro-*p*-benzoquinone, and 5-iodo-*m*-xylene from Aldrich were used as received. Iodomesitylene, 4-iodo-1,2,3-trimethylbenzene, and iodopentamethylbenzene were prepared by iodination of the parent hydrocarbon with iodine monochloride/ZnCl₂ in acetic acid.⁵⁷ 2-Ethynylmesitylene and 5-ethynyl-*m*-xylene were prepared by reaction of (trimethylsilyl)acetylene with 2-iodomesitylene and 5-iodo-*m*-xylene, respectively, according to the literature procedure.¹⁸ Dichloromethane and tetrahydrofuran were purified using published procedures.⁵⁸

Preparation of Diarylacetylenes. The substituted acetylenes were prepared by the palladium-catalyzed coupling of the corresponding aryl iodides and arylacetylenes in diethylamine.¹⁸ The products were purified by flash chromatography and recrystallized from ethanol. Characteristic physical data for **3,5-dimethyl-1-(phenylethynyl)benzene**, **FX** are the following: mp 45 °C; ¹H NMR δ 2.30 (s, 6H), 6.96 (s, 1H), 7.17 (s, 2H), 7.29–7.34 (m, 3H), 7.45–7.58 (m, 2H); ¹³C NMR δ 21.09, 88.67, 88.70, 122.81, 123.42, 128.05, 128.28, 129.25, 130.17, 131.54, 137.85; GC-MS *m/z* 206 (M^+ , 100). Anal. Calcd for C₁₆H₁₄: C, 93.16; H, 6.84. Found: C, 92.92; H, 6.89. The characterization of the other diaryl acetylenes is included in the Supporting Information. ¹H and ¹³C NMR spectra were recorded in CDCl₃ on a General Electric QE-300 NMR spectrometer and the chemical shifts are reported in ppm units downfield from tetramethylsilane. UV–vis absorption spectra were recorded on a Hewlett-Packard 8453 diode-array spectrometer. Infrared spectra were recorded on a Nicolet 10DX FT spectrometer. Gas chromatography was performed on a Hewlett-Packard 5890A series gas chromatograph equipped with a HP 3392 integrator. GC-MS analyses were carried out on a Hewlett-Packard 5890 chromatograph interfaced to a HP 5970 mass spectrometer (EI, 70 eV). Melting points were performed on a Mel-Temp (Laboratory Devices) apparatus and are uncorrected. All elemental analyses were carried out by Atlantic Microlab Inc., Norcross, GA.

Cyclic Voltammetry of the Diarylacetylenes. Cyclic voltammetry (CV) was performed on a BAS-100A Electrochemical Analyzer. The CV cell was of an airtight design with high vacuum Teflon valves and

Viton O-ring seals to allow an inert atmosphere to be maintained without contamination by grease. The working electrode consisted of an adjustable platinum disk embedded in a glass seal to allow periodic polishing (with a fine emery cloth) without changing the surface area (~1 mm²) significantly. The SCE reference electrode and associated salt bridge were separated from the catholyte by a sintered glass frit. The counter electrode consisted of a platinum gauze that was placed ~3 mm from the working electrode. The cyclic voltammetric measurements were carried out in dry dichloromethane containing 0.1 M tetra-*n*-butylammonium hexafluorophosphate as supporting electrolyte and 5 × 10⁻³ M toluene, under an argon atmosphere. All cyclic voltammograms were recorded at the sweep rate of 100 mV s⁻¹ and were IR compensated. The potentials were referenced to SCE which was calibrated with added ferrocene (5 × 10⁻³ M) as the internal standard. The 1-electron oxidation of this series of acetylenes was irreversible in all cases, and thus the uncorrected anodic peak potentials are as follows: **FX**, 1.69; **TX**, 1.61; **FH**, 1.54; **FM**, 1.54; **XX**, 1.57; **TH**, 1.45; **XM**, 1.48; **XM**, 1.46; **FP**, 1.46 V vs SCE.

Photoinduced Coupling of Diarylacetylenes with 2,6-Dichlorobenzoquinone. General Procedure. A dichloromethane solution of **DB** (53 mg, 0.1 M) and **FX** (63 mg, 0.1 M) was prepared (under an argon atmosphere) in a quartz cuvette fitted with a Teflon stopcock. An identical solution was prepared in a similar cuvette, sealed under argon, and wrapped in aluminum foil to serve as the “dark” control. The two cuvettes were then placed in a clear Dewar flask filled with water at 25 °C and the reaction cuvette was irradiated with focused light from a medium-pressure mercury lamp (500 W) passed through an aqueous IR filter and an ESCO 410 nm filter. This ensured that the quinone itself was excited and not the diarylacetylene. After 22 h, both solutions were analyzed by GC with *N*-phenylphenothiazine as internal standard. The reactants, **DB** and **FX**, were recovered unchanged from the dark control solution; however, the irradiated solution comprised a mixture of the starting compounds and the corresponding quinone methide product. The solvent was evaporated and the crude mixture subjected to flash chromatography. The quinone methide was isolated in 88% yield based on the reacted starting material (62% conversion, see Table 1). The product was recrystallized from acetonitrile and characteristic physical data for the two quinone methide isomers are as follows: **1'-(3,5-Dimethylphenyl)-1'-benzoyl-1-methylene-3,5-dichlorocyclohexa-2,5-dien-4-one**, **1a**: mp 191–192 °C; ¹H NMR δ 2.36 (s, 6H), 7.08 (s, 2H), 7.13 (s, 1H), 7.31 (d, *J* = 2.4 Hz, 1H), 7.46–7.53 (m, 3H), 7.72 (d, *J* = 2.4 Hz, 1H), 7.93 (br d, *J* = 7.2 Hz, 2H); ¹³C NMR δ 21.29, 127.51, 127.52, 129.20, 129.35, 130.10, 132.95, 134.14, 134.40, 134.88, 135.22, 139.23, 157.91, 173.04, 194.78; GC-MS *m/z* 382 [M^+ ($2 \times ^{35}\text{Cl}$), 36], 347 (100), 105 (99). Anal. Calcd for C₂₂H₁₆Cl₂O₂: C, 68.97; H, 4.21. Found: C, 68.71; H, 4.31. The minor isomer **1b** was identified by GC-MS *m/z* 382 [M^+ ($2 \times ^{35}\text{Cl}$), 29], 105 (100). The spectroscopic characterization of the other quinone methides is described in detail in the Supporting Information.

Charge-Transfer Absorption Spectra of Diarylacetylene Donors with 2,6-Dichlorobenzoquinone. A dichloromethane solution of **DB**, 0.015 M, was prepared in a quartz cuvette under an argon atmosphere, and the UV–vis absorption spectrum of the pale yellow solution was recorded. **FX** (30 mg, 0.15 M) was added and the absorption spectrum of the resultant pale orange solution recorded. The absorption spectrum of the quinone was digitally subtracted from the latter spectrum and the difference spectrum referred to as the charge-transfer (CT) absorption spectrum. To determine the formation constant of the CT complex, the respective concentrations of the quinone and the diarylacetylene were chosen such that the diarylacetylene was added incrementally in large excess (e.g. [**DB**] = 0.015 M and [**FX**] ranging from 0.15 to 0.7 M). The charge-transfer absorptions at the spectral maxima (A_{CT}) were determined and the Benesi–Hildebrand procedure²⁷ applied to calculate the formation constant, K_{EDA} , and the extinction coefficient, ϵ_{CT} , of the EDA complex formation according to eq 7. Thus the quotient of the quinone concentration and the absorbance at the maximum was plotted against the reciprocal of the donor concentration and the intercept equated to (ϵ_{CT})⁻¹ and the slope to ($K_{\text{EDA}}\epsilon_{\text{CT}}$)⁻¹. The values are listed in Table 2.

Charge-Transfer Photoinduced Coupling of Diarylacetylenes with 2,6-Dichlorobenzoquinone. General Procedure. Two identical

(56) Time-resolved CIDNP studies by Eckert and Goetz¹⁶ led to similar conclusions for the Paterno–Büchi coupling of quinones and anetholes.

(57) Andrews, L. J.; Keefer, R. M. *J. Am. Chem. Soc.* **1957**, 79, 1412.

(58) Perrin, D. D.; Armarego, W. L. F.; Perrin, D. R. *Purification of Laboratory Chemicals*, 2nd ed.; Pergamon: New York, 1980.

(59) Spagnola, P.; Martelli, G.; Tiecco, M. *J. Chem. Soc. (B)* **1970**, 1413.

0.1 M dichloromethane solutions of **FX** and **DB** were prepared in quartz cuvettes and sealed under an atmosphere of argon. One cuvette was wrapped in aluminum foil to serve as “dark” control, and the two cuvettes were placed side-by-side in a Dewar flask at 25 °C. The reaction cuvette was irradiated with focused light from a medium-pressure mercury lamp passed through an aqueous IR filter and a Corning 530-nm cutoff filter. This cutoff filter ensured the exclusive excitation of the EDA complex. After 48 h, both solutions were analyzed by quantitative GC using an internal standard. The dark control remained unreacted while the conversions and yields of the charge-transfer activated reactions are shown in Table 3.

Quantum Yields for the Photocoupling of Diarylacetylenes and 2,6-Dichlorobenzoquinone. (a) **Excitation at $\lambda_{\text{exc}} = 440$ nm.** The quantum yields were measured with the aid of a medium pressure (500 W) mercury lamp that was focused through an aqueous IR filter followed by an ESCO 440 ± 7.5 nm narrow band-pass interference filter. The output of the lamp was determined with a freshly prepared potassium ferrioxalate actinometer, as described by Calvert and Pitts.³² This measurement was performed at room temperature using a 1-cm square cuvette fitted with a Schlenk adapter. The same cuvette was then filled under a flow of argon with a dark orange dichloromethane solution of **TX** (2×10^{-1} M) and **DB** (2×10^{-1} M). At these concentrations, the absorbance at 440 nm remained above 2 throughout the irradiation, and thus no correction for transmitted light was necessary. After 4 h of irradiation, the solution was diluted with dichloromethane and the contents quantified by GC. The only product formed was **2**. The quantum efficiencies for the formation of the corresponding quinonemethide are shown in representative results in Table 4.

(b) **Excitation at $\lambda_{\text{exc}} = 580$ nm.** The quantum yields were measured with the same lamp focused through an aqueous IR filter followed by an ESCO 580 ± 7.5 nm narrow band-pass interference filter. The output of the lamp was determined using potassium reineckate salt.³³ This measurement was performed at room temperature using a 1-cm square cuvette fitted with a Schlenk adapter. The same cuvette was then filled under a flow of argon with a dark orange dichloromethane solution of **TX** (2×10^{-1} M) and **DB** (2×10^{-1} M) to ensure that the absorbance at 580 nm remained above 2 throughout the irradiation (and no correction for transmitted light was necessary).

After 4 h of irradiation, the solution was diluted with dichloromethane and the contents quantified by GC. The only product formed was the quinone methide **2**, and the quantum efficiency for formation is listed in Table 4.

Time-Resolved Absorption Spectra from Photoexcitation of Diarylacetylenes and 2,6-Dichlorobenzoquinone. (a) **Direct Excitation of 2,6-Dichlorobenzoquinone ($\lambda_{\text{exc}} = 355$ nm).** The direct excitation of the quinone was performed with a Q-switched Nd³⁺:YAG laser with a 10-ns pulse as described previously.³⁴ Dichloromethane solutions of **DB** and **FM** were prepared, under an argon atmosphere, in a 1-cm quartz cuvette fitted with a Teflon stopcock. The concentrations of the components were adjusted such that the absorbance at the excitation wavelength of $\lambda = 355$ nm was between 0.5 and 0.8.

(b) **Charge-Transfer Excitation ($\lambda_{\text{exc}} = 532$ nm).** The charge-transfer excitation of the EDA complex between **FM** and **DB** was performed with a mode-locked Nd³⁺:YAG laser using the second harmonic at 532 nm as previously described.³⁴ The concentrations of the components were adjusted such that the absorption at the excitation wavelength (532 nm) was between 0.25 and 0.4 while also ensuring that the absorbance at 400 nm was below 1.2. This was imperative since the transient absorption displayed a strong signal centered at 430 nm, and this signal was diminished and poorly defined when there was excessive ground-state absorption at these wavelengths.

Acknowledgment. We thank T. M. Bockman for many helpful suggestions, S. V. Lindeman for crystallographic assistance, and the R. A. Welch Foundation and the National Science Foundation for financial support.

Supporting Information Available: Figure 2, PLUTO perspective of quinone methide **8b**, Figure 3, UV–vis spectral changes upon the incremental addition of tolyl(mesityl)acetylene to a dichloromethane solution of **DB** and **TM**, and spectroscopic data for the synthesized arylacetylenes and the quinone methide products (7 pages). See any current masthead page for ordering and Internet access instructions.

JA9727530